# Precise Orbit Determination of High-Earth Elliptical Orbiters Using Differenced Doppler and Range Measurements

J. A. Estefan
Navigation Systems Section

*Recent advances in Deep Space Network station calibration methods have led to renewed interest in the use of differenced Doppler and range data types for interplanetary navigation. This article describes an orbit determination error analysis of the performance of these differenced data types when used with conventional two-way Doppler for precise navigation of High-Earth Orbiters. Three highly elliptical Earth orbits are investigated, with apogee heights on the order of 20,000 km, 70,000 km, and 156,000 km. Results indicate that the most significant navigational accuracy improvements, relative to the performance obtained from two-way Doppler alone, are achieved for the lowest altitude orbit by using differenced Doppler measurements with two-way Doppler (assuming that spacecraft onboard downlink antennas have no ground footprint limitation in the near-apogee regime). In the case of the two higher altitude orbits, accuracy improvements over Doppler-only performance, although less dramatic, are also achieved when differenced range measurements are combined with two-way Doppler.*

## I. Introduction

As NASA's commitment to supporting national and international High-Earth Orbiter (HEO) missions continues to evolve, it is becoming increasingly apparent that the NASA/JPL Deep Space Network (DSN) will be tasked with providing tracking and navigational support, particularly for the orbiting radio astronomy platforms planned for launch as early as 1995. The DSN is proceeding with the implementation of a dedicated HEO subnetwork of 10-m antennas for this purpose.[1]

[1] J. Ovnick, "Orbiting VLBI Subnet C/D Review," Presentation Viewgraphs, Jet Propulsion Laboratory, Pasadena, California, April 3, 1991.

A host of tracking techniques and data types have been investigated for possible use in HEO mission support. The most common data types that are expected to receive widespread use are two-way Doppler and two-way range. High-accuracy interferometric and differential techniques, such as very long-baseline interferometry (VLBI) and $\Delta$VLBI, as well as Global Positioning System (GPS)-based tracking have also received much attention [1,2]. One technique that has been suggested is a differenced one-way range (DOR) by multiple frequency phase measurements, which modulates the transmission of the spacecraft so that cycle ambiguities can be eliminated and which measures only the phase differences [3] (not to be confused with $\Delta$DOR, in which an observation of an ex-

tragalactic radio source is also used). It has also been suggested that postprocessed VLBI science data be used to improve the accuracy of the orbit [4], but this would only be possible for radio astronomy platforms and is not likely to benefit the orbit determination process unless real time, or at least, near-real-time correlation is possible. Other, more esoteric methods have been investigated, including the use of satellite laser ranging systems and onboard microaccelerometers. The advantages and disadvantages of these tracking methods have been discussed in greater detail in [5].

A data type that is geometrically equivalent to DOR, yet somewhat less cumbersome to implement operationally, is two-way minus three-way range (differenced range). Analogously, two-way minus three-way Doppler (differenced Doppler) can also be employed. These data types are usually referred to as "quasi-VLBI" data because they provide information about the spacecraft position and velocity similar to that provided by VLBI. Although less accuracy can be achieved than with VLBI, differenced Doppler or range data can be made available for navigational purposes faster than data from the DSN VLBI system. Until recently, differenced range was not thought to provide adequate accuracy for orbit determination due to large systematic errors associated with the data, in particular, clock offsets between co-observing stations. However, this method is becoming more attractive as better calibration systems become available. A recent analysis has shown that improvements in DSN ranging system calibration accuracies, together with clock offset and other calibration data derived from the GPS, could theoretically determine spacecraft angular coordinates to 30–90 nrad accuracy [6]. A similar investigation of the use of differenced Doppler for orbit determination, based on analysis of the 8.4-GHz (X-band) data acquired from the Magellan spacecraft, showed that differenced Doppler might deliver 50–100 nrad spacecraft angular accuracy, except for spacecraft within about 10 deg of the celestial equator [7]. Results from these analyses are encouraging enough to warrant investigation of these data types for use in HEO mission support.

This article presents an orbit determination accuracy assessment for an HEO mission set by using two-way range, differenced Doppler, and differenced range measurements together with conventional two-way Doppler. Three different HEO missions are studied, each of which is taken from the orbiting-VLBI (OVLBI) radio astronomy platform set: the Japanese VLBI Space Observatory Program (VSOP); the Soviet RADIOASTRON Project; and the International VLBI Satellite (IVS). Orbital characteristics for each mission are defined, with associated ground tracks and DSN view periods provided. An array of numerical error covariance analyses are performed to evaluate orbit determination accuracies achievable with different data strategies. A detailed description of the assumptions used for tracking data simulation and error modeling is also provided, along with a discussion of observable formulation and downlink footprint limitations, as well as a description of the orbit determination error-modeling parameters. In summary, a performance assessment is provided for each mission based on the numerical results generated during the study.

## II. Mission Orbital Characteristics

A set of sample orbit parameters for VSOP and RADIOASTRON are summarized in Tables 1 and 2 (initial spacecraft ephemerides are referenced to Earth mean equator and equinox of date). Based on these orbital characteristics, each orbiter will trace repeatable ground tracks and VSOP will experience a nodal regression and apsidal rotation of roughly 180 deg per year due to Earth oblateness. The RADIOASTRON orbit will maintain a "fixed" perigee since its orbital inclination is taken to be near the critical value of 63.4 deg; the ground track required to remain constant with about a 24-hr period. A ground-track profile and DSN view periods for VSOP are shown in Figs. 1(a) and 1(b) for a typical 24-hr period.[2]

The sample RADIOASTRON orbit optimizes ground coverage over the Soviet Union, but has limited visibility from the DSN, with the exception of Madrid. To use differenced data types, at least two ground stations must simultaneously "view" the spacecraft for some interval of time, but the nominal orbital geometry does not permit a view period overlap for any DSN intercontinental baseline. Therefore, for this analysis, the longitude of the ascending node is shifted westward to 145 deg, which enables an overlap between Madrid and Goldstone. The corresponding ground track and DSN view periods for this shifted orbit are shown in Figs. 2(a) and 2(b).

In the case of the IVS, mission design remains in the early stages of development; a "nominal" orbit has yet to be clearly defined. There does exist an array of suggested orbital geometries ranging from a moderate-altitude (~25,000 km) to a high-altitude (~40,000 km) orbit, even an "ultra-high" altitude (~150,000 km) orbit has been suggested. A set of four orbit phases was selected in an ear-

[2] The labels DSCC 10, DSCC 40, and DSCC 60 in this and subsequent figures represent the Deep Space Communications Complexes (DSCCs) at Goldstone, California; near Canberra, Australia; and near Madrid, Spain, respectively.

lier IVS orbit determination study [8], but only the ultra-high altitude phase is considered here since the moderate- and high-altitude orbit cases are similar geometrically to VSOP and RADIOASTRON. The orbital parameters are summarized in Table 3, with the corresponding ground-track and DSN view periods shown in Figs. 3(a) and 3(b).

## III. Assumptions for Numerical Error Covariance Analysis

### A. Observable Development

The general model for the range observable used in the Orbit Analysis and Simulation Software (OASIS) package is defined by

$$\rho \equiv r + \tau_T + \tau_I + \tau_C \tag{1}$$

where

$r$ = distance between the spacecraft and Earth-based tracking station[3]

$\tau_T$ = delay due to troposphere

$\tau_I$ = delay due to ionosphere

$\tau_C$ = delay due to clock offset calibration errors

A detailed mathematical description of observable models and their associated partial derivatives (partials) is provided in *OASIS Mathematical Description.*[4] The range rate, which is proportional to the Doppler observable, is determined by taking the time derivative of the range observable given in Eq. (1). The studies presented here for two-way measurements assume that appropriate linear combinations of the one-way measurements described by Eq. (1) can be formed for purposes of conducting error analyses. These assumptions apply to observable formulation and computation of the partials; moreover, round-trip light time corrections are omitted in the formulation of the observations and partials (even though this capability does exist) since these corrections are normally reserved for interplanetary studies. Partials for ionospheric refraction are omitted in this analysis since it is expected that the sensitivity due to tropospheric path delay will be the major propagation media effect due to the high operating frequencies proposed for OVLBI (i.e., 8–15 GHz).

[4] S. C. Wu, W. I. Bertiger, J. S. Border, S. M. Lichten, R. F. Sunseri, B. G. Williams, P. J. Wolff, and J. T. Wu, *OASIS Mathematical Description, V. 10*, JPL D-3139 (internal document), Jet Propulsion Laboratory, Pasadena, California, April 1, 1986.

Constructing an observable for differenced Doppler/range amounts to differencing a two-way and a three-way measurement. The resulting observable is a by-product of differencing the downlink signals of each participating Earth-based tracking station over a common view period (see Fig. 4). Mathematically, this can be expressed as

$$\Delta\dot{\rho}(\Delta\rho) = \underbrace{\dot{\rho}_{1u}(\rho_{1u}) + \dot{\rho}_{1d}(\rho_{1d})}_{\text{2-way measurement}} - \underbrace{[\dot{\rho}_{1u}(\rho_{1u}) + \dot{\rho}_{2d}(\rho_{2d})]}_{\text{3-way measurement}} \tag{2}$$

$$= \dot{\rho}_{1d}(\rho_{1d}) - \dot{\rho}_{2d}(\rho_{2d})$$

where

$\dot{\rho}_{1u}(\rho_{1u})$ = uplink Doppler/range measurement from DSN station 1 to the spacecraft

$\dot{\rho}_{1d}(\rho_{1d})$ = downlink Doppler/range measurement from the spacecraft to DSN station 1

$\dot{\rho}_{2d}(\rho_{2d})$ = downlink Doppler/range measurement from the spacecraft to DSN station 2

### B. Tracking Data Simulation

For the error analyses, two-way 8.4-GHz (X-band) Doppler data were taken to be the primary data type and were collected continuously from two Deep Space Stations (DSSs), at different intervals, throughout the course of a single orbit arc.[5] The two stations were chosen so that a region of overlap existed in which differenced Doppler and range measurements could also be acquired.

To account for data noise, the Doppler was weighted with a 1-$\sigma$ measurement uncertainty of 0.1 mm/sec over a 60-sec integration time. The data weight ($1/\sigma^2$) was adjusted according to the minimum elevation at the station, and data points below 10-deg local horizon were omitted. In certain cases, two-way 2.3-GHz (S-band) range data were acquired continuously along with Doppler but sampled at a rate of one point every 240 seconds. These data were also weighted for minimum elevation, and the 1-$\sigma$ measurement uncertainty was taken to be 15 cm. As with Doppler, range data were collected only when the spacecraft was considered in-view—when the station elevation angle is greater than 10 deg.

Differenced Doppler and range measurements were collected (assuming a three-way link) only in the near-

[5] It is expected that the VSOP mission will use a 15-GHz link; the analysis in this article is meant as an illustrative case using the VSOP orbit, not as a specific application for the mission.

apoapsis region of the orbit. Differenced Doppler measurements were sampled over a 60-sec integration time with elevation corrections. The 1-$\sigma$ measurement uncertainty was assumed to be 0.15 mm/sec—50 percent more noisy than two-way Doppler data. Differenced range measurements were weighted (also according to minimum elevation) with 1-$\sigma$ measurement uncertainty of 22.5 cm, and with a data point acquired every 2 minutes.[6]

Four data strategies were assumed for each OVLBI mission: two-way Doppler only, two-way Doppler plus two-way range, two-way Doppler plus differenced Doppler, and two-way Doppler plus differenced range.

An important caveat to note is that it may not be possible to construct differenced Doppler/range measurements due to the limited ground signature (footprint) of the parabolic downlink antenna designs expected for the OVLBI. This could be a major obstacle if these data types are sought to be employed operationally, especially for the large intercontinental baselines of the DSN and with high link frequencies. Table 4 shows a small sample of antenna footprints (computed from beamwidth = frequency/diameter) that assume a parabolic downlink antenna operating at 8.4 GHz (X-band). (Note that the Goldstone–Madrid baseline is roughly 8,600 km in length, while the Goldstone–Canberra baseline is about 10,600 km.)

It is clear from the table that the expected slant ranges for the VSOP are not nearly large enough to facilitate the acquisition of three-way data for any DSN intercontinental baseline; not to mention the fact that the 15-GHz link further reduces the size of the ground footprint. For RADIOASTRON, it may be possible to acquire three-way data from a Goldstone–Madrid baseline if a small (~0.25-m diameter) downlink antenna is employed and if data are collected near the apoapsis regions of the orbit. Of the three orbits considered in this study, the ultra-high altitude IVS orbit clearly would be most suitable for the acquisition of three-way data. Perhaps for future HEO missions, a variety of antenna-link designs and configurations (e.g., multiple, independently pointable antennas) will be considered.

[6] These may be slightly more "conservative" estimates of the measurement uncertainty; if independent and random measurements were assumed for the differenced data types investigated here, one could argue that the measurement uncertainty for differenced Doppler/range could be determined $\sigma_{\Delta\dot{\rho}}(\sigma_{\Delta\rho}) = \sqrt{2}\sigma_{\dot{\rho}}$ ($\sqrt{2}\sigma\rho$). In this case, the one-sigma uncertainties for differenced Doppler/range would be approximately 0.14 mm/sec and 21.2 cm, respectively.

## C. Orbit Determination Modeling Errors[7]

The modeling of error sources was performed in essentially the same manner for all three OVLBI missions and was based on the current and expected future performance of the spacecraft and the DSN. The fundamental error-modeling assumptions used in this analysis were based on Konopliv's earlier work,[8] but were somewhat modified and expanded for completeness.

The error-modeling parameters are broken down into two categories: estimated and considered. The random data noise characteristics addressed in Section III.B are summarized in Table 5, along with the estimated parameters, considered parameters, and associated sigmas.

**1. Estimated Parameters.** The estimated parameters were chosen to account for mismodeling of spacecraft nongravitational accelerations and calibration errors for certain data types. Random accelerations due to solar radiation pressure (SRP) and gas leaks were treated as stochastic processes and were estimated along with the spacecraft trajectory.

For the VSOP, RADIOASTRON, and the IVS spacecraft, the area-to-mass ratios were taken to be 0.04, 0.03, and 0.10 $m^2kg^{-1}$, respectively. (The small area-to-mass ratio for VSOP occurs because the onboard VLBI antenna is expected to be nearly 80 percent transmissive, whereas the the small ratio for RADIOASTRON results from the large mass, 4,000 kg, of the spacecraft). The SRP specular and diffuse reflectivity coefficients were designated stochastic variables, and the stochastic model for process noise was taken to be a first-order Markov colored noise model (exponentially correlated process) with steady state sigmas equivalent to 10 percent of the maximum attainable a priori values. Time constants were chosen to be roughly equivalent to the orbital period in each case (1/4 day for the VSOP, 1 day for RADIOASTRON, and 3 days for the IVS). A batch-sequential, factorized Kalman filter was used in the estimation process, with batch sizes for each of the aforementioned missions of 1 hr, 3 hr, and 6 hr, respectively.

Gas leak accelerations (in each spacecraft body-fixed axis) were estimated stochastically with steady state sig-

[7] A quick semantic note: The words *error* and *uncertainty* are used interchangeably throughout the text and, as such, they are intended to be synonymous; moreover, an error, in this context, is intended to imply uncertainty in measurement, not a mistake or blunder.

[8] A. Konopliv, "Preliminary Orbit Determination Analysis for the VSOP Mission," JPL Interoffice Memoranda 314.4-648 and 314.4-667 (internal documents), Jet Propulsion Laboratory, Pasadena, California, February 9 and July 20, 1989.

mas of $10^{-12}$ km/sec$^2$, and time constants were assumed to be 1 day for the VSOP and RADIOASTRON and 3 days for the IVS. The batch sizes were taken to be equivalent to the SRP batch sizes.

To account for the effects of station-frequency offset-calibration errors on differenced Doppler data, a bias parameter was added to these measurements. The bias parameter was estimated as a constant parameter with 1-$\sigma$ uncertainty of the total a priori offset calibration value of 0.02 mm/sec. In the case of two-way range, a bias parameter was added for each DSS receiver to account for clock offsets and signal path delays. Similarly, for differenced range, a clock offset or signal path delay bias parameter was added. The 1-$\sigma$ uncertainty of the total a priori offset calibration value was taken to be 300 cm (~20 nsec). These uncertainties are representative of present-day capabilities. In the future, it is expected that GPS-based calibration methods will substantially reduce these uncertainties.

**2. Considered Parameters.** A *consider* parameter is treated by the filter as an unmodeled systematic error and may significantly affect the error statistics of the estimated parameter set. The total error covariance accounts for the consider variances as well as the variances computed by the filter, so as not to understate the predicted navigational performance. The considered parameters used in this study accounted for systematic errors in station locations, offset in the geocenter, gravity modeling, and tropospheric path delay.

Station uncertainties include both a relative component and an absolute (geocentric) component. The relative component refers to DSN-site–DSN-site uncertainty (measured accurately by VLBI); the geocentric component refers to a common error in locating the DSN sites with respect to the Earth mass center (VLBI is insensitive to this component). Conservative equatorial station location errors of 50–75 cm were assumed;[9] the relative error (station–station) being about 30 cm. For the $z$-direction, 10-cm relative and 1-m geocentric errors were assumed. Analysis indicates that the expected accuracy of the geocenter can be determined to better than 10 cm by using GPS-based measurements [9]. The majority of this analysis assumes that no such calibrations were available, again, for conservatism; the only exception being one special case in which GPS-based measurements were indeed assumed for calibrating the limiting error sources associated with each data type. This special case is further described in the next section.

Gravity-error modeling included the Earth's Newtonian gravitational parameter (GM) and an 8×8 reduced-order GEM-T2 gravity field obtained from NASA–Goddard Space Flight Center's 50×50 field [10]. Uncertainty of the GM was taken to be 1 part in $10^8$, while the formal sigmas for the GEM-T2 gravity field harmonics were used and assumed to be uncorrelated.[10]

The wet and dry components of error contribution due to tropospheric path delay were considered with zenith uncertainties of 4 cm and 1 cm, respectively (based on present-day values from a seasonal model).

Atmospheric drag and Earth albedo (radiation pressure reflected from Earth) were omitted from the error-modeling process because their effects were shown to contribute less than 1 cm to the total orbit determination error in an earlier analysis [8].

## IV. Performance Assessment

The orbit determination accuracy results described here are expressed in terms of uncertainty in spacecraft position and velocity. All stated results represent root-mean-square (rms) or 1-$\sigma$ performance statistics, since the batch-sequential filter in this analysis used linear unbiased estimation methods. The filter-generated computed covariance was combined with consider parameter sensitivities to construct the total or *full consider covariance*, which was then mapped forward in time to produce a time history of propagating error sources and navigational performance for four data strategies (Doppler only, Doppler plus two-way range, Doppler plus differenced Doppler, and Doppler plus differenced range). The covariance was mapped ahead for a duration of 24 hr in the case of the VSOP and RADIOASTRON orbits, and 72 hr in the case of the IVS orbit.

### A. VSOP Orbit

The accuracy statistics for VSOP position and velocity uncertainties are shown in Figs. 5(a) and 5(b). These figures represent the total uncertainty over time, in a root-sum-square (rss) sense, of all vector components,

[9] T. Moyer, "Station Location Sets Referred to the Radio Frame," JPL Interoffice Memorandum 314.5-1334 (internal document), Jet Propulsion Laboratory, Pasadena, California, February 24, 1989.

[10] Another, and perhaps more common, approach to gravity field mismodeling is to assume a "lumped sum" uncertainty of a fraction (say 50 percent) of two *differenced* gravity fields (e.g., GEM-10 and GEM-L2). This is usually the method of choice when computational disk space and processing time are at a premium.

i.e., radial (altitude), transverse (down-track), and normal (cross-track), which account for the computed plus consider errors.

Two-way Doppler and range were collected only during the first passes at Madrid (00:17 to 03:57 hr) and Goldstone (06:16 to 09:04 hr), a little over 7 hr in all; no other stations were used for data acquisition. To construct differenced Doppler and differenced range measurements, a 90-min three-way link between 07:34 and 09:04 hr was assumed for a Madrid–Goldstone baseline (baseline slant ranges: ~18,000–24,000 km). The performance of the Doppler-only and Doppler-plus-range solutions was very similar throughout the reconstruction and prediction phases of the propagation cycle. By augmenting the Doppler-only data set with a relatively short pass of differenced Doppler or differenced range data, a dramatic improvement in orbit determination performance resulted, which suggests that, by using differenced Doppler data over the data arc, there is about a 59-percent improvement in position performance and about a 78-percent improvement in velocity performance. When differenced range data are used, there is about a 43-percent improvement in position determination and about a 63-percent improvement in velocity performance.

Figure 6 represents a "snapshot" of performance statistics for position and velocity taken at the initial apogee crossing and at the first perigee passage, respectively. The total uncertainty is broken down into the orthogonal components of radial, transverse, and normal error. Again, the Doppler-only and Doppler-plus-range measurements yield similar characteristics, while the differenced measurements improve results more dramatically. It is especially interesting to note that the Doppler plus differenced-Doppler measurements were significantly better able to determine the out-of-plane (normal) component than the other data strategies investigated.

For the same snapshot event, a breakdown of individual error sources is provided (see Fig. 7). The computed statistics represent the estimated or formal filter results and are frequently referred to as data noise contributions. The differenced Doppler measurements appear to yield the best performance with respect to each error source. The important observation, however, is that, by augmenting the two-way Doppler data with either differenced Doppler or differenced range data, the effect of the tropospheric uncertainty, which is the dominant error source here, is substantially reduced. This behavior occurs because line-of-sight data types, such as two-way Doppler and range, are very sensitive to tropospheric zenith-delay calibration errors, whereas differenced Doppler and range data types are relatively less sensitive to the calibration errors. Another important observation is the power of the differenced data types for reducing velocity uncertainty in the near-perigee regime, again, with the tropospheric uncertainty contribution being dramatically reduced.

### B. RADIOASTRON Orbit

In some respects, the covariance results for the RADIOASTRON position uncertainty resemble those of the VSOP, despite different orbital characteristics. However, this is not true in the case of velocity uncertainty. Results for velocity performance are omitted due to the less than 10-percent difference among all four data strategies investigated (see Table 6 for a summary of all results). Accuracy statistics for position uncertainty are provided and summarized in Fig. 8.

Two-way Doppler and range data were collected from Goldstone and Madrid between 00:34 and 13:43 hr and 14:00 to 23:34 hr, respectively. This amounted to nearly a 23-hr data arc—substantial coverage, indeed. Differenced Doppler and differenced range measurements were constructed for a 4-hr Goldstone–Madrid baseline between 09:42 and 13:42 hr (baseline slant ranges: ~71,000–74,000 km). The results indicate about a 6-percent improvement in position determination when range data are included with the Doppler; this is clearly evident in the region ±6 hr of apoapsis. The augmented differenced Doppler case yields about a 7-percent improvement, but begins to degrade late in the day. Measuring Doppler plus differenced range data appears to be the best strategy in terms of orbit determination performance throughout the entire data arc. Results indicate about a 13-percent improvement over Doppler-only solutions.

Performance statistics taken at the initial apogee crossing in terms of orthogonal components and individual error sources are shown in Figs. 8(b) and 8(c), respectively. Here, all four data strategies yield similar performances in terms of the radial and transverse components, with the exception of the normal component, which was better determined by using differenced Doppler or differenced range data.

From the error-breakdown chart, Fig. 8(c), the dominant error sources appear to be data noise, station locations, and troposphere. The differenced data strategies, particularly differenced range, seem to reduce the uncertainty in the troposphere, whereas for the VSOP orbit, the differenced Doppler helped to reduce the uncertainty in the troposphere better than the other data types. This phenomenon reflects the fact that there is greater information content in the differenced Doppler measurements

for the lower altitude, highly elliptical orbiters, since the data are very sensitive to the spacecraft's orbital motion. The differenced range information content is greater for the higher altitude elliptical orbiters because the data are more sensitive to orbital geometry than dynamics.

### C. IVS Orbit

The IVS ultra-high altitude orbit case (67-hr orbit) offers an interesting problem in terms of scheduling tracking passes. For this study, the argument of perigee and longitude of ascending node were "optimized" to provide substantial data coverage, particularly for the northern hemisphere stations. As in the RADIOASTRON cases, the covariance results for velocity uncertainty amounted to less than a 15-percent difference for all four data strategies, which translates to only ~0.13 mm/sec improvement at best; therefore, these statistics are not shown. The position uncertainty is certainly dependent upon the assumed data strategy, and accuracy statistics are provided in Fig. 9.

Several long passes of two-way Doppler and range data can be obtained from Madrid and Goldstone for this orbit. The tracking schedule is taken to be: 00:38 to 14:46 hr (Madrid) and 15:00 to 23:06 hr (Goldstone) for the first day; 04:56 to 01:44 hr (Goldstone) for the second-to-third day; and 02:00 to 17:48 hr (Madrid) for the third day, a total of ~59 hr. Ten hours of three-way data were acquired for a Madrid–Goldstone baseline ±5 hr either side of apogee (baseline slant ranges: ~148,000–151,000 km). The results show that the Doppler-plus-range strategy yields the best performance during the early part of the orbit arc (i.e., for the first day), but then begins to degrade at the start of the second day. For this case, about a 13-percent improvement in performance resulted between $P_0 + 6$ hours and $P_1 - 6$ hours, where $P_0$ represents the initial perigee point (at epoch) and $P_1$ represents the first perigee passage (end of the orbit arc). When differenced Doppler and differenced range data are used, better performance clearly results throughout most of the reconstruction phase, with differenced range data yielding the best results, about a 20-percent improvement in performance, while differenced Doppler provided only about a 14-percent improvement.

Figures 9(b) and 9(c) give the accuracy statistics for all four data strategies in terms of orthogonal components and error characteristics. As with the RADIOASTRON cases, the radial component is determined about equally as well for the four data strategies, and only slightly better for Doppler-plus-range data. However, unlike RADIOASTRON, the transverse component is better determined with the augmented data. The normal component is, again, best determined with the differenced data types.

Limiting error sources for this case are seen to be data noise and station location uncertainties, with the data noise component for the two-way Doppler-only case dominating all other error sources. This should not be surprising because of the long data arcs used in this case. Effects of gravity mismodeling are, as expected, negligible because of the high-altitude phase of this orbit (~150,000 km). Unlike the VSOP and RADIOASTRON, the data strategy of Doppler plus range appears to be most sensitive to tropospheric calibration errors.

To gain insight into what orbit determination accuracies can be achieved by using these radiometric data types together with GPS-based ground observations for measuring and calibrating the major systematic error sources, a second set of numerical covariance analysis runs was made for IVS. Results are shown in Fig. 10, again with velocity omitted because of the relatively insignificant difference in performance among data strategies (23-percent improvement at best, which translates to ~0.16 mm/sec).

For this study, a tighter error budget was assumed with respect to the observing platform and propagation media errors, as well as the biases associated with each data type. Specifically, relative station location uncertainties were reduced to 7 cm (each component), the wet zenith troposphere delay to 2 cm, and the geocenter offset to 10 cm. These values are still considered to be rather conservative, especially for a mid-to-late 1990s time frame.[11] The a priori frequency bias was then taken to be 0.003 mm/sec (1 part in $10^{14}$), while a priori biases due to clock offset and signal path delays were taken to be 2 nsec (60 cm).

The same tracking passes were assumed in the earlier case. The Doppler-only solution is improved over the original Doppler-only solution, and the augmented data strategies also yield better performance than in the original case: about 29-percent improvement for Doppler plus range data, 32-percent improvement for Doppler plus differenced-Doppler data, and 39-percent improvement for Doppler plus differenced-range data.

In terms of orthogonal components, the radial error component is again about the same for all strategies, but transverse and normal components were significantly better determined by using the augmented data types. Clearly, when used in concert with the augmented data

[11] S. Lichten, private communication, Tracking Systems and Application Section, Jet Propulsion Laboratory, Pasadena, California.

types assumed in this analysis, the GPS-based ground observations reduced the major systematic error sources substantially enough, see Fig. 10(c), that performance becomes limited only by the quality of the data. Similar performance improvements were evident in earlier orbit determination analyses of the actual VSOP and RADIOASTRON missions.[12,13]

These results are very encouraging because they suggest that radiometric data types, such as two-way Doppler, can deliver precise, orbit determination accuracies when augmented with differenced data types and GPS-based ground-calibration data. It is hoped that such a ground-calibration system will become operational not only for support of future HEO missions, but also for deep-space missions.

Table 6 gives a summary chart of orbit determination accuracy results (rss total uncertainty in position and velocity) for all the different data strategies and missions investigated. A range of statistics is displayed which indicates the rms or 1-$\sigma$ orbit determination accuracy results accumulated over the reconstruction phases (data arcs) of a single orbit arc for each mission. For this analysis, the relative improvement is difficult to quantify because it varies over different phases of the orbit, and knowledge at some points may be more important than at others. Table 6 attempts to quantify the improvement in two ways, giving both the range in uncertainties and the average (percentage) improvement over the data arcs. The actual values used to produce the percentages of improvement were computed by integrating each error curve over the data arc to obtain the total area relative to the total area of the reference data strategy of two-way Doppler only.

## V. Remarks

In this analysis, long two-way Doppler passes were used, which amounted to obtaining all possible data available from two ground telemetry sites. This, of course, may not be realizable in an operational setting without a dedicated ground network of antennas. Nevertheless, by utilizing all the Doppler data available and comparing the resulting performance with that obtained from relatively short passes of differenced data, one can ascertain the true power of the differenced data types. The results suggest that the more two-way data available, the less the influence of the differenced data on the resulting orbit determination accuracy. However, it is not yet clear if the improvement is strictly a function of the orbital motion/geometry or due to the relative lengths of the data arcs; most likely, it is a combination of both (recall that the VSOP orbit determination results using differenced Doppler/range yielded the most dramatic results). This makes intuitive sense since the VSOP maintained a lower altitude than its counterparts, RADIOASTRON and IVS, and the lower the altitude, the greater the parallax between the co-observing stations; hence, information content of the data is increased. It could be that if substantial coverage (i.e., two-way Doppler data) cannot be obtained due to other antenna demands, use of even a limited amount of differenced data would provide increased orbit determination accuracy. The availability of GPS calibrations may assume greater significance if the data quantities are limited.

It is also important to note that only east–west baselines were investigated for this study. This was not intentional, but was a result of the fact that the orbital characteristics of the cases examined were simply better suited for east–west baselines. It is not yet clear whether better performance can be achieved with north–south baselines.

The downlink antenna footprint limitation can be of serious consequence operationally, especially if high link frequencies (~8 GHz and higher) are to be used. Therefore, future missions may require the use of two downlink antennas to obtain the possible performance improvements seen here.

## VI. Conclusions

An orbit determination analysis was performed for a set of three different orbits being considered as orbiting radio astronomy (OVLBI) platforms to investigate the utility of differenced Doppler and range measurements. The orbital characteristics were described along with a discussion of the assumptions used for numerical error covariance calculations. The covariance analyses were performed by using a factorized Kalman filter to estimate a set of governing parameters and to compute the sensitivity of the estimated parameters to a set of unmodeled considered parameters that were treated as systematic error sources. Orbit determination accuracy statistics were calculated for all three orbits with an additional case reflecting the use of GPS-based ground observations for calibrating all radiometric data types investigated (two-way Doppler/range and differenced Doppler/range).

[12] C. S. Christensen and J. A. Estefan, "Orbit Determination Capability for VSOP Using DSN Doppler Tracking," JPL Interoffice Memorandum 314.5-1424 (internal document), Jet Propulsion Laboratory, Pasadena, California, March 15, 1990.

[13] C. S. Christensen and J. A. Estefan, "Orbit Determination Capability for Radioastron Using DSN Doppler Tracking," JPL Interoffice Memorandum 314.5-1448 (internal document), Jet Propulsion Laboratory, Pasadena, California, June 4, 1990.

Results indicate that for the VSOP orbit, an accuracy improvement of up to 59 percent was achieved by using two-way Doppler plus differenced Doppler for position determination, and up to 78-percent improvement in velocity determination by using the same data strategy. These were, by far, the most dramatic results seen in the analysis. For the RADIOASTRON and the IVS orbits, the relative improvement in velocity by using two-way range measurements or even differenced measurements was rather insignificant. However, up to 20-percent improvement in position determination was evident when differenced range measurements were used to augment the two-way Doppler measurements. The power of the differenced data types was even more evident when GPS-based ground calibrations were assumed to measure and calibrate the limiting systematic error sources. In the case of the IVS orbit, orbit determination accuracy improved by roughly 39 percent in position and 23 percent in velocity.

In exploring potential tracking methods for highly precise (submeter) orbit determination, earlier orbit determination analyses [8] focused on exploiting conventional two-way Doppler tracking together with GPS-based tracking methods, which included ground-based calibration data as well as onboard flight receivers. The results suggested that the two tracking techniques complemented each other extremely well throughout the orbit arcs, and it would be interesting to investigate what accuracies might be achieved when differenced Doppler and differenced range measurements are used in the tracking processes as well.

## Acknowledgments

The author is indebted to Jim Ulvestad for providing the essential material regarding downlink footprint limitations and for his critical review of the draft report. His comments and suggestions proved invaluable in completing this work effort. A warm thanks to Sam Thurman for inspiring this work effort; and to him, Carl Christensen, and Steve Lichten for their careful review of the subject matter.

## References

[1] R. B. Frauenholz and J. Ellis, "Orbit Determination of Highly Elliptical Earth Orbiters Using VLBI and ΔVLBI Measurements," *TDA Progress Report 42-75*, vol. July–September 1983, Jet Propulsion Laboratory, Pasadena, California, pp. 1–13, November 15, 1983.

[2] T. P. Yunck, W. G. Melbourne, and C. L. Thornton, "GPS-Based Satellite Tracking System for Precise Positioning," *IEEE Transactions on Geoscience and Remote Sensing*, vol. GE-23, pp. 450–457, July 1985.

[3] S. Gorgolewski, "Precise RADIOASTRON Baseline Determination," paper presented at the discussion meeting on the "RADIOASTRON project: Navigation, Astrometry, Geodesy Aspects" of the SGO-IKI Joint Working Group, Satellite Geodetic Observatory, Penc, Hungary, February 27–March 3, 1989.

[4] I. Fejes, T. Borza, Sz. Mihály, and L. Szánthó, "Orbit Determination Accuracy Improvement by Space-VLBI Observables as Tracking Data," paper presented at the IAG General Meeting, Symposium 101: Global and Regional Geodynamics, Edinburgh, Scotland, August 3–5, 1989.

[5] I. Fejes, ed., *Precise Orbit Determination of RADIOASTRON*, report prepared by the RADIOASTRON Navigation, Astrometry, and Geodesy (NAG) Group for the 8th RADIOASTRON Review meeting, ver. 29, Satellite Geodetic Observatory, Penc, Hungary, April 1989.

[6] S. W. Thurman, "Deep-Space Navigation with Differenced Data Types, Part I: Differenced Range Information Content," *TDA Progress Report 42-103*, vol. July–September 1990, Jet Propulsion Laboratory, Pasadena, California, pp. 47–60, November 15, 1990.

[7] S. W. Thurman, "Deep-Space Navigation with Differenced Data Types, Part II: Differenced Doppler Information Content," *TDA Progress Report 42-103*, vol. July–September 1990, Jet Propulsion Laboratory, Pasadena, California, pp. 61–69, November 15, 1990.

[8] S. M. Lichten and J. A. Estefan, *High Precision Orbit Determination for High-Earth Elliptical Orbiters Using the Global Positioning System*, paper AIAA 90-2954, AIAA/AAS Astrodynamics Conference, Portland, Oregon, August 20–22, 1990.

[9] R. P. Malla and S. C. Wu, "The Geocenter Estimation Results Using GPS Measurements," *GPS '90* (in press), September 3–7, 1990, paper presented at the Second International Symposium on Precise Positioning with the Global Positioning System, Ottawa, Canada, September 1990.

[10] J. G. Marsh, F. J. Lerch, B. H. Putney, T. L. Felsentreger, B. V. Sanchez, S. M. Klosko, G. B. Patel, J. W. Robbins, R. G. Williamson, T. L. Engelis, W. F. Eddy, N. L. Chandler, D. S. Chinn, S. Kapoor, K. E. Rachlin, L. E. Braatz, and E. C. Pavlis, "The GEM-T2 Gravitational Model," *Journal of Geophysical Research*, vol. 95, no. B13, pp. 22,043–22,071, December 10, 1990.

**Table 1. Sample orbit parameters for the Japanese Very Long Baseline Interferometry Space Observatory**

| Parameter | Value |
|---|---|
| Epoch | |
| Date | January 1, 1995 |
| Time | $00^h:00^m:00^s.0000$ UTC |
| Initial spacecraft ephemeris | |
| Semi-major axis | 16,878 km |
| Eccentricity | 0.5629 |
| Inclination | 46.0° |
| Argument of perigee | 0.0° |
| Longitude of ascending node | 0.0° |
| Mean anomaly | 0.0° |
| Additional parameters | |
| Perigee height | 1,000 km |
| Apogee height | 20,000 km |
| Orbit period | 6.06 hr |

**Table 2. Sample orbit parameters for the Soviet RADIOASTRON Project**

| Parameter | Value |
|---|---|
| Epoch | |
| Date | August 1, 1993 |
| Time | $00^h:00^m:00^s.0000$ UTC |
| Initial spacecraft ephemeris | |
| Semi-major axis | 42,378 km |
| Eccentricity | 0.802303 |
| Inclination | 65.0° |
| Argument of perigee | 285.0° |
| Longitude of ascending node | 200.0° |
| Mean anomaly | 0.0° |
| Additional parameters | |
| Perigee height | 2,000 km |
| Apogee height | 70,000 km |
| Orbit period | 24.10 hr |

**Table 3. Orbit parameters for ultra-high altitude International VLBI Satellite Orbit**

| Parameter | Value |
|---|---|
| Epoch | |
| Date | January 1, 1999 |
| Time | $00^h:00^m:00^s.0000$ UTC |
| Initial spacecraft ephemeris | |
| Semi-major axis | 83,878 km |
| Eccentricity | 0.86435 |
| Inclination | 63.0° |
| Argument of perigee | 270.0° |
| Longitude of ascending node | 120.0° |
| Mean anomaly | 0.0° |
| Additional parameters | |
| Perigee height | 11,378 km |
| Apogee height | 156,378 km |
| Orbit period | 67.14 hr |

**Table 4. Approximate parabolic antenna footprint, km, for 8.4-GHz (X-band) downlink**

| Slant Range, km | Antenna diameter, m | | |
|---|---|---|---|
| | 0.25 | 0.50 | 0.75 |
| 60,000 | 8,571 | 4,286 | 2,857 |
| 80,000 | 11,429 | 5,714 | 3,810 |
| 100,000 | 14,286 | 7,143 | 4,762 |
| 120,000 | 17,143 | 8,571 | 5,714 |
| 140,000 | 20,000 | 10,000 | 6,667 |
| 160,000 | 22,857 | 11,429 | 7,619 |

**Table 5. Orbit determination error model parameters**

| Parameter | Uncertainty, $1\sigma$ |
|---|---|
| Random data noise | |
| Two-way Doppler | 0.1 mm/sec |
| Two-way range | 15 cm |
| Differenced Doppler | 0.15 mm/sec |
| Differenced range | 22.5 cm |
| Estimated parameters (a priori) | |
| Spacecraft | |
| Position | 1,000 m |
| Velocity | 1 km/sec |
| Stochastic accelerations | |
| Solar radiation pressure | 10% of max |
| Gas leaks | $10^{-9}$ m/sec$^2$ |
| Biases | |
| Frequency offset | 0.02 mm/sec |
| Clock offset/signal path delay | 300 cm (20 nsec) |
| Considered parameters | |
| Gravity | |
| Earth's GM | GM$\times 10^{-8}$ |
| Harmonics | 8×8 field (GEM-T2) |
| DSN station coordinates | |
| Crust fixed | |
| Spin radius and longitude | 50–75 cm |
| Z-height | 10 cm |
| Geocenter-Z | 1 m |
| Zenith troposphere delay | |
| Wet | 4 cm |
| Dry | 1 cm |

**Table 6. 1-σ orbit determination accuracy comparison for different data strategies**

| Data Strategy | RSS Position Uncertainty, m, and Relative Percentage Improvement | | | |
|---|---|---|---|---|
| | VSOP | RADIOASTRON | IVS | IVS + GPS Calibrations |
| Doppler-only versus | 6.0–18.1 | 2.8–11.8 | 3.1–13.5 | 2.3–10.6 |
| Doppler + range | 5.6–16.8<br>6% | 2.5–11.0<br>6% | 2.8–11.9<br>13% | 1.8–7.5<br>29% |
| Doppler + Δ Doppler | 2.3–7.0<br>59% | 2.5–11.0<br>7% | 3.0–11.8<br>14% | 2.2–8.4<br>32% |
| Doppler + Δ range | 3.1–9.9<br>43% | 2.4–10.3<br>13% | 3.0–11.5<br>20% | 2.2–8.2<br>39% |
| Data Strategy | RSS Velocity Uncertainty, cm/sec, and Relative Percentage Improvement | | | |
| | VSOP | RADIOASTRON | IVS | IVS + GPS Calibrations |
| Doppler-only versus | 0.18–0.85 | 0.030–0.33 | 0.020–0.24 | 0.015–0.21 |
| Doppler + range | 0.17–0.78<br>7% | 0.030–0.30<br>6% | 0.016–0.21<br>13% | 0.011–0.17<br>22% |
| Doppler + Δ Doppler | 0.04–0.18<br>78% | 0.030–0.32<br>5% | 0.015–0.24<br>10% | 0.011–0.21<br>20% |
| Doppler + Δ range | 0.06–0.24<br>63% | 0.028–0.31<br>10% | 0.014–0.23<br>15% | 0.010–0.20<br>23% |

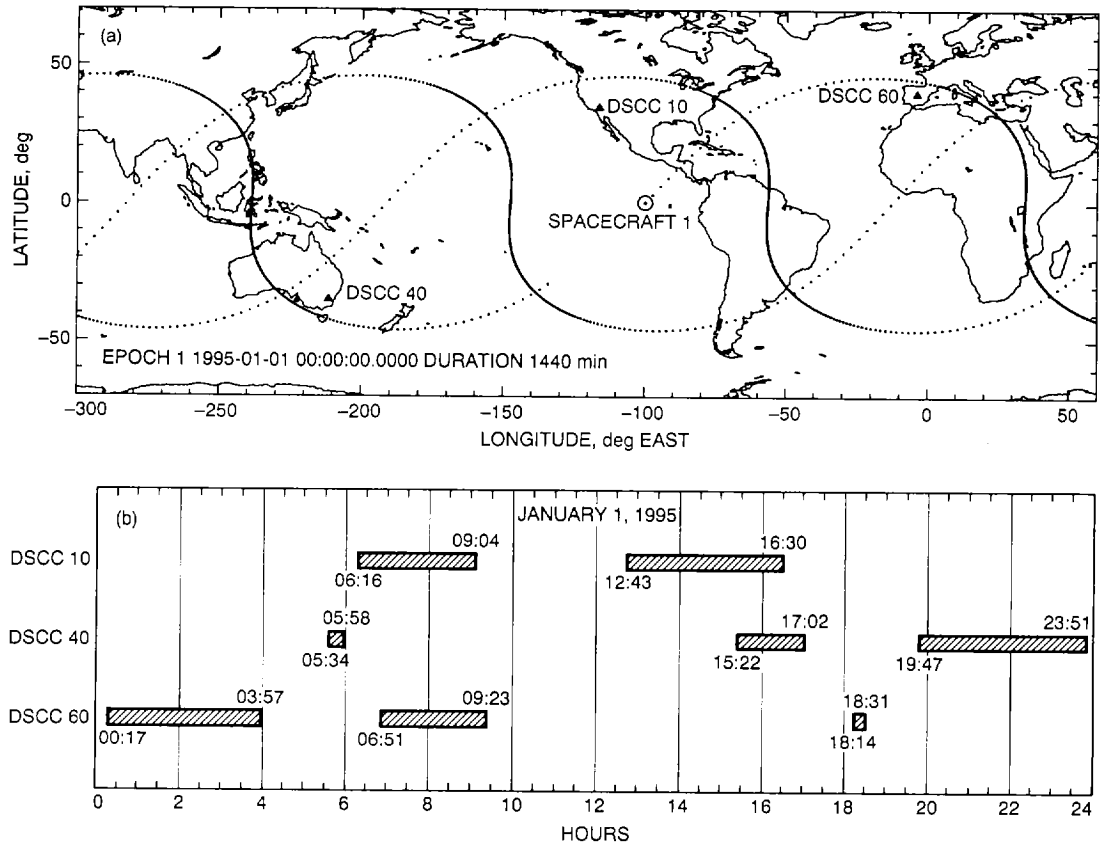


**Fig. 1. DSN visibility profile for the VSOP sample orbit: (a) spacecraft ground track (1-min spacing); (b) ground network view periods (spacecraft rise/set times).**

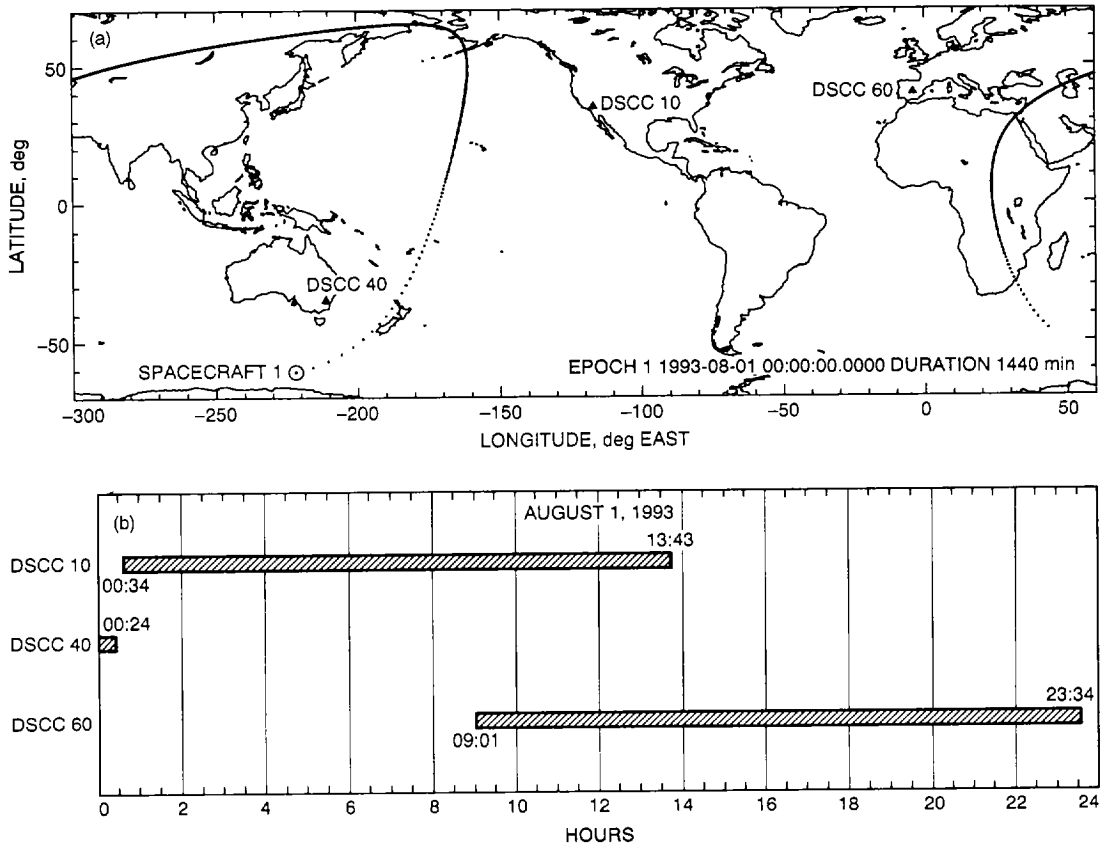


**Fig. 2. DSN visibility profile for the RADIOASTRON shifted orbit: (a) spacecraft ground track (1-min spacing); (b) ground network view periods (spacecraft rise/set times).**

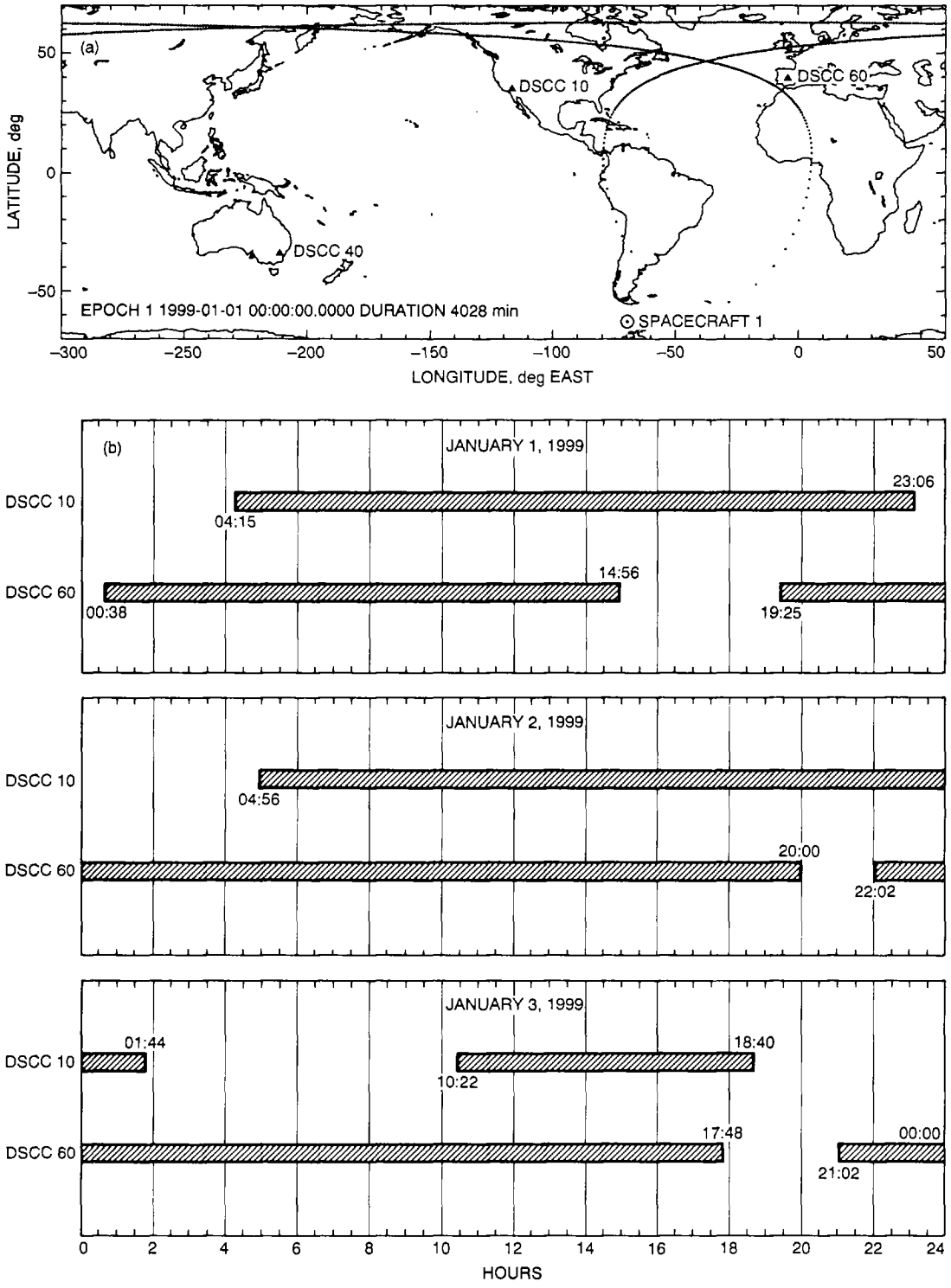


**Fig. 3. DSN visibility profile for the ultra-high altitude IVS orbit: (a) spacecraft ground track (5-min spacing); (b) ground network view periods (spacecraft rise/set times).**

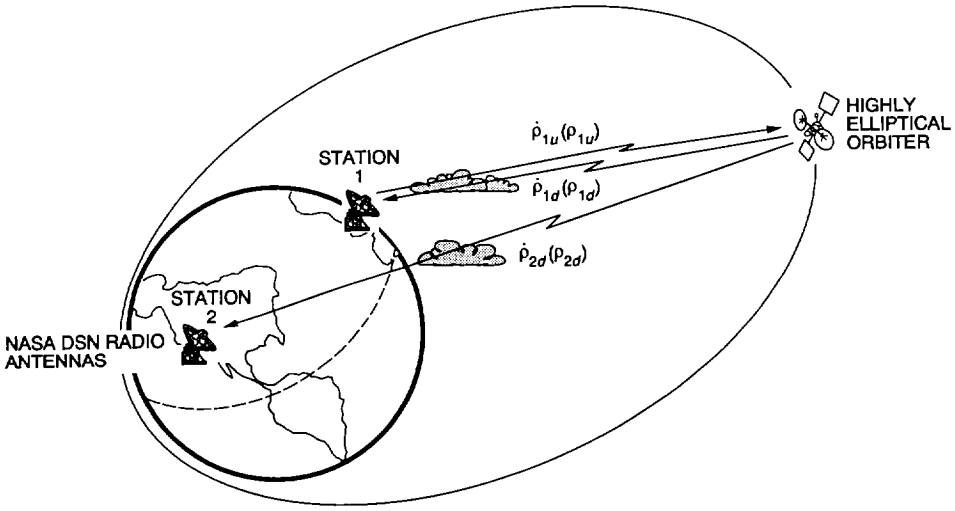


**Fig. 4. Differenced Doppler/range acquisition scheme.**

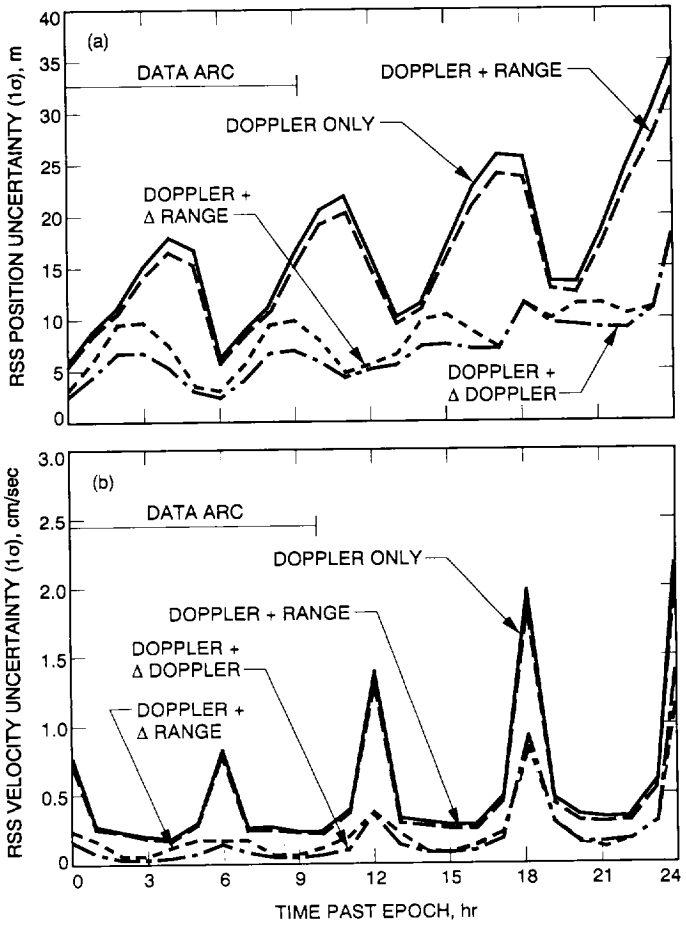


**Fig. 5. VSOP 1-$\sigma$ orbit determination accuracy statistics for: (a) expected RSS total position uncertainty; (b) expected RSS total velocity uncertainty.**

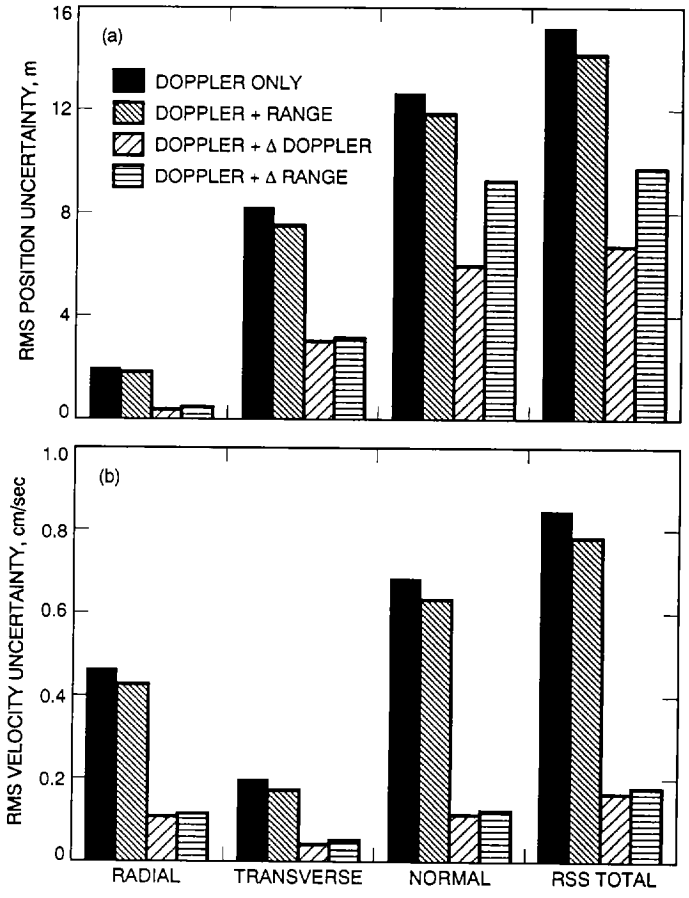


**Fig. 6. VSOP 1-$\sigma$ orbit determination accuracy statistics for: (a) expected position uncertainty at initial apogee crossing in terms of orthogonal components; (b) expected velocity uncertainty at first perigee passage (6 hr past epoch) in terms of orthogonal components.**

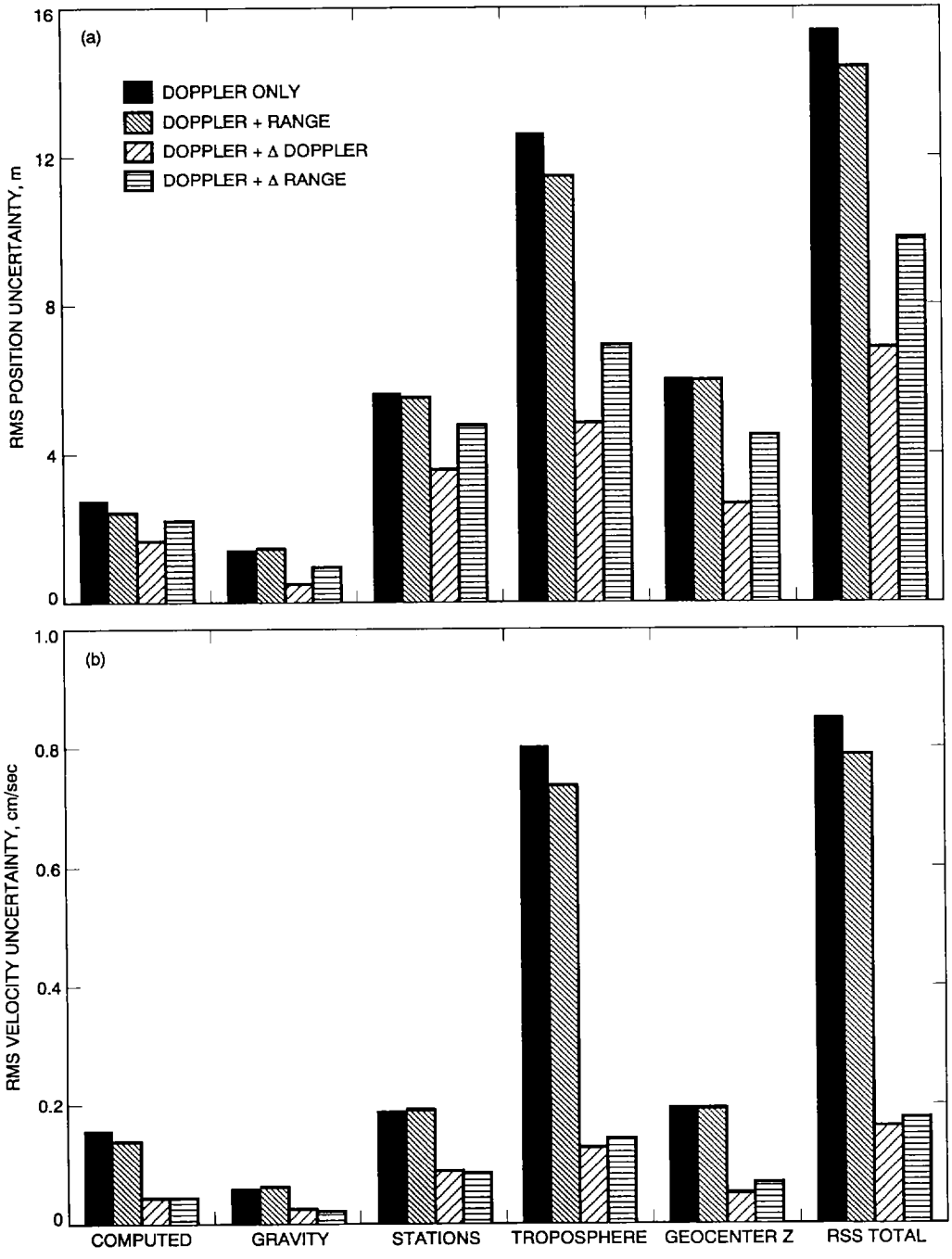


**Fig. 7. VSOP 1-$\sigma$ orbit determination accuracy statistics for: (a) expected position uncertainty at initial apogee crossing in terms of individual error sources: (b) expected velocity uncertainty at first perigee passage (6 hr past epoch) in terms of individual error sources.**

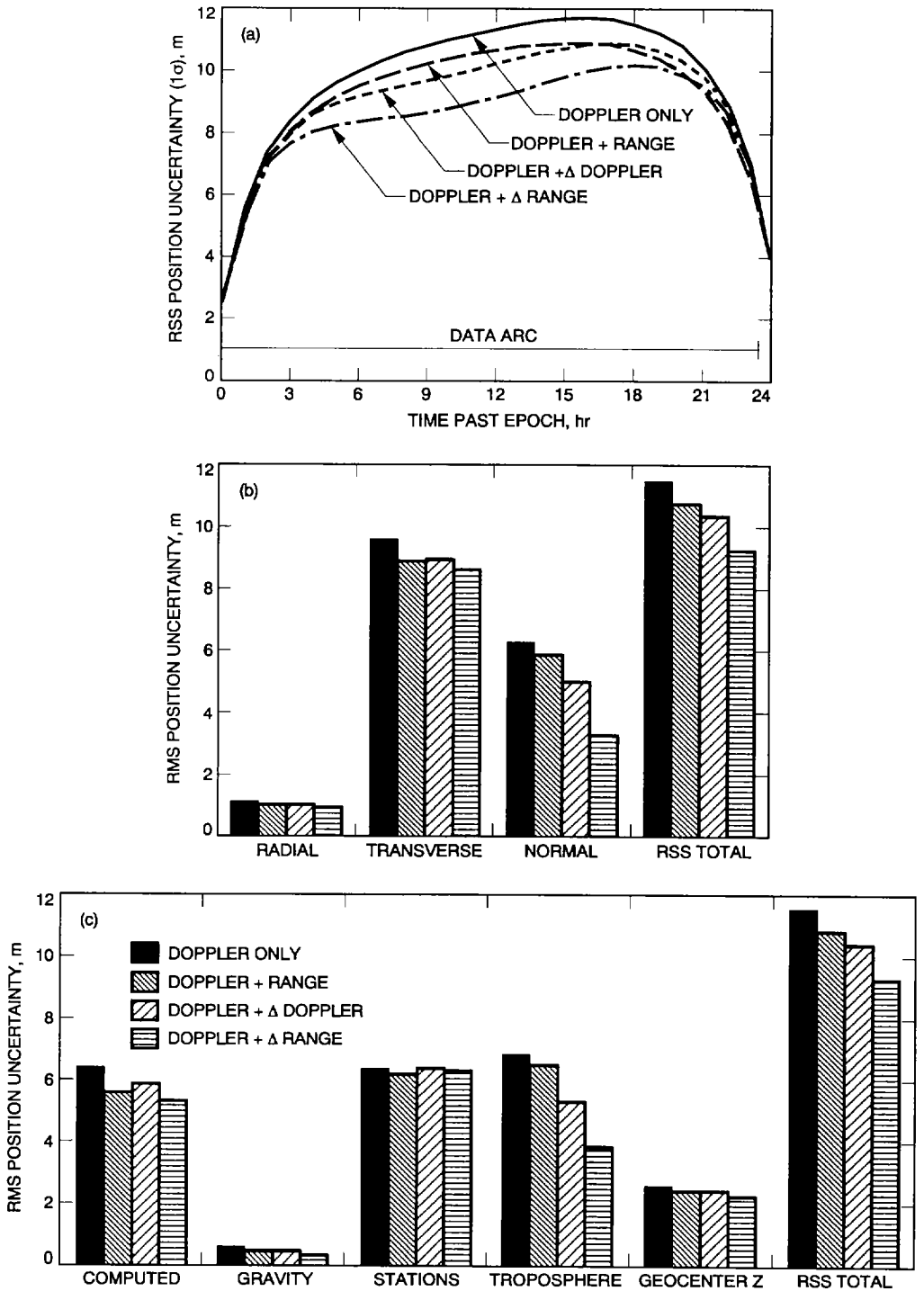


**Fig. 8. RADIOASTRON 1-$\sigma$ orbit determination accuracy statistics for: (a) expected RSS total position uncertainty; (b) expected position uncertainty at initial apogee crossing in terms of orthogonal components; (c) expected position uncertainty at initial apogee crossing in terms of individual error sources.**

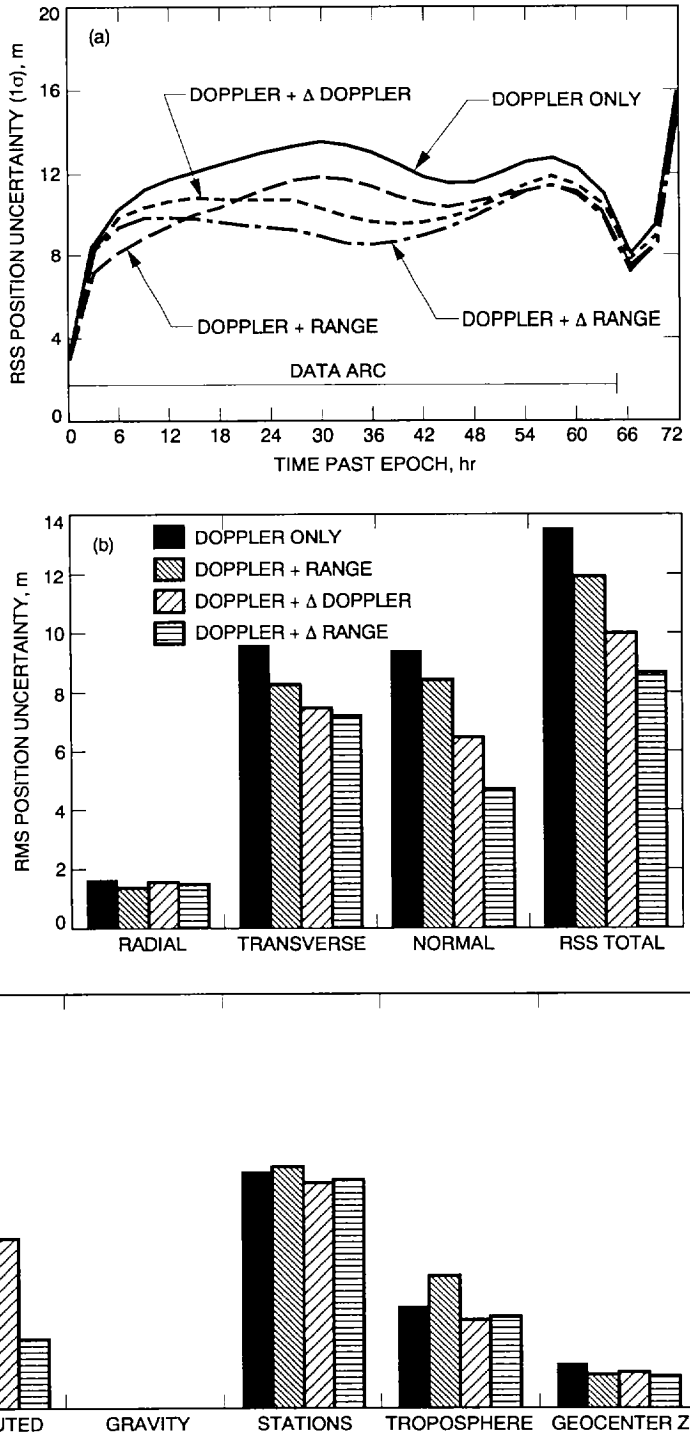


**Fig. 9. IVS 1-$\sigma$ orbit determination accuracy statistics for: (a) expected RSS total position uncertainty; (b) expected position uncertainty near initial apogee crossing in terms of orthogonal components; (c) expected position uncertainty near initial apogee crossing in terms of individual error sources.**

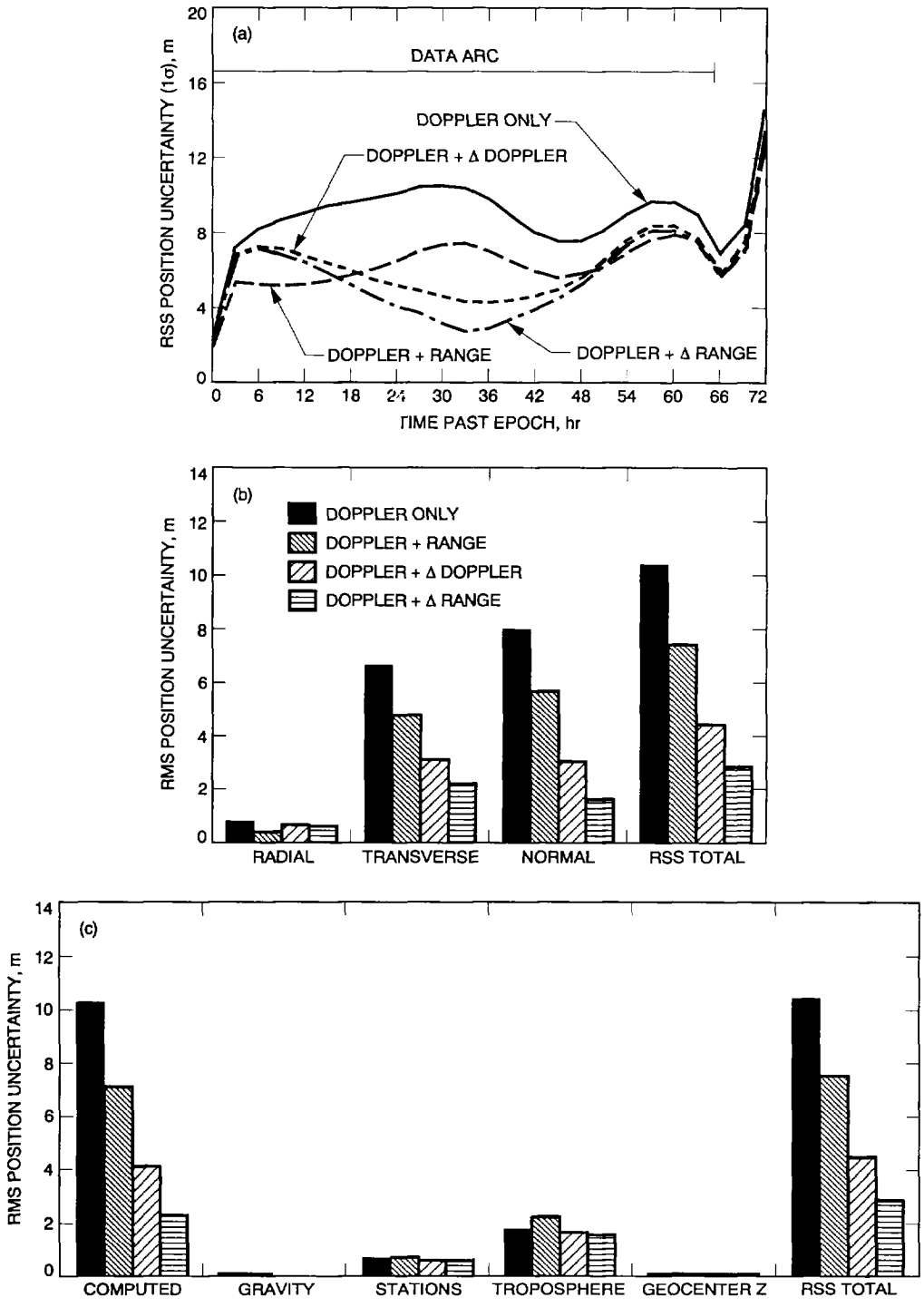


**Fig. 10. IVS 1-$\sigma$ orbit determination accuracy statistics using GPS-based ground observations for: (a) expected RSS total position uncertainty; (b) expected position uncertainty near initial apogee crossing in terms of orthogonal components; (c) expected position uncertainty near initial apogee crossing in terms of individual error sources.**